International Journal of Advanced Technology in Engineering and Science
Vol. No.3, Special Issue No. 01, September 2015
www.ijates.com
ijates
ISSN 2348 - 7550

DYNAMIC ANALYSIS ON BALLOONING MOTION OF STRESS-SOFTENEDRUBBER STRING

N. Gautam

Assistant Professor, Department of Mechanical Engineering, VEC Lakanpur, Sarguja University, Ambikapur (C.G.), (India)

ABSTRACT

In this paper the effect of stress-softening on the hyperelastic rubber string is investigated by using neo-Hookean material model. The microstructural damage is characterized by an exponential softening function that depends on the current magnitude of the strain–energy function and its maximum previous value in a deformation of the virgin material. This theoretical damage model is developed in order to provide a description of an idealized form of the Mullins effect for various deformation states. Tension and stretch distribution along the balloon height can be predicted. Air drag is particularly useful in controlling the shape and size of the balloon.

It is assumed that the extent of stretch is limited to an upper bound value of 3, i.e. $\lambda \leq 3$. Since the simplest possible constitutive behavior of a hyperelastic, homogenous and incompressible rubber material in this range is given by neo-Hookean model, which we shall use in our present work. A solution to the boundary value problem is obtained by shooting method for the ballooning motion of a neo-Hookean string. It has been observed that preconditioning makes the rubberlike material softer and one needs comparatively less length to form a steady state balloon for a given tension, and the softer string shows more ballooning radius by stretching the balloon more in comparison to that prevailing in the virgin string. Stress-softening is found to be more effective in lesser values of speed. A good correlation is found when experimental results are compared with theoretical results.

Keywords: Hyperelastic, Mullins Effect, Neo-Hookean, Stress-Softening, Virgin.

Nomenclature

a	String radius at fixed eyelet
e_1,e_2,e_3	Rotating coordinate system
H	Ballooning height
h	Nondimensoinalised balloon height
i, j, k	Indices
l_0	Nondimensoinalisedundeformed length of the balloon
γ	Nondimensoinalised parameter, ratio of Young's modulus to inertial stress
Ω	Angular velocity
S_0,S_1,S_2	Arc length inreference configuration, steady state configuration and final configuration respectively
$\tilde{t}$	Time

t	Nondimensoinalised time
P	Tension in the string
p	Nondimensoinalised parameter, ratio of tension in string to inertial force
ρ	Density of string
λ	Stretch
s	Nondimensoinalised arc length coordinate
Y	Young's Modulus
$\kappa_0,\kappa_1,\kappa_2$	Configuration of the system
A	Area of the string
X,Y,Z	Stationary Coordinate system
x,y,z	Nondimensoinalised coordinates
r	Normalized position vector
r	Balloon radius at rotating eyelet
λ_e	Stretch at fixed eyelet
Δ_0	Undeformed length parameter
P_e	Nondimensoinalised tension at eyelet
ε	Error
B	Left Cauchy-Green deformation tensor
F	Deformation gradient
b	Softening parameter
Θ	Maximum previous strain intensity
θ	Current strain intensity
W	Strain energy density function.

I. INTRODUCTION

As far as the elasticity of rubber is concerned there are some fundamental assumptions that are adopted in the phenomenological theory: the material is (a) hyperelastic, (b) isotropic, and (c) incompressible. Hyperelasticitymeans that the properties of the material are described in terms of a strain-energy functionand it refers to those materials which can experience large elastic deformation. The elasticity of a solid can vary depending on its state of deformation. Metals will soften and polymers may stiffen as they are deformed to failure levels. It happensonly when the deformation is infinitesimally small that elastic moduli can be considered constant. Yet, many existing theories model fracture using linear elasticity, regardless of the fact that materials will experience extreme deformations at crack tips. Here we show that the elastic behavior observed at large deformations, hyperelasticity can play a vital role in the dynamics of fracture, and that linear theory is incompetent of fully capturing all fracture phenomena. Isotropy (relative to a stress-free configuration) is a very good approximation in most circumstances and is almost invariably used by practitioners. Incompressibility is an idealization, justified by the fact that the shear modulus of the material is very much smaller than the bulk modulus (typically the ratio is of order 10^{-4}) and volume changes can be neglected except in extreme situations where the hydrostatic stress is very large. For the most part isotropy and incompressibility are assumed in

practical applications. The strain energy is a function of the deformation gradient **F** (relative to some fixed reference configuration).

The hyperelastic, homogenous, incompressible rubber like material models include several forms of strain energy functions, such as Neo-Hookean, Ogden [1], Arruda-Boyce [11]and James-Guth [12]. To account for large deformation in such materials we consider symmetric left Cauchy-Green deformation tensor **B**, given as

$$B = FF^T \qquad (1)$$

where $F=\frac{\partial x}{\partial X}$ is the deformation gradient, in which x is the position of particle in deformed configuration and X is the position of particle in undeformed or reference configuration. The strain energy density function is the function of three invariants of the strain tensor **B** and they are defined as

$$I_1 = trB, I_2 = \frac{1}{2}(I_1^2 - trB^2), I_3 = \det B \qquad (2)$$

For incompressible materials, $I_3=1$. Thus the strain energy density function depends only on first two invariantsfor any isochoric deformation i.e. $W=W(I_1,I_2)$ and the Cauchy stress response is written as

$$T = -pI + 2\left(\frac{\partial W}{\partial I_1}\right)B + 2\left(\frac{\partial W}{\partial I_2}\right)B^{-1} \qquad (3)$$

wherep is the undetermined hydrostatic pressure appearing from the incompressibility constant and $\partial W/\partial I_1 \geq 0, \partial W/\partial I_2 \leq 0$. The principal directions at a point are eigenvectors of**B**, and the positive square roots of its eigenvalues are the principal stretches $\lambda_1,\lambda_2,.\lambda_3$ and the invariants can be expressed in terms of these as

$$I_1 = \lambda_1^2 + \lambda_2^2 + \lambda_3^2, I_2 = \lambda_1^2\lambda_2^2 + \lambda_2^2\lambda_3^2 + \lambda_3^2\lambda_1^2, \quad I_3 = \lambda_1^2\lambda_2^2\lambda_3^2 = 1. \qquad (4)$$

II. MULLINS STRESS-SOFTENING EFFECT

When a rubber specimen is loaded uniaxially at a very low strain rate, unloaded, and loaded again, the load required to produce same deformation in the second loading cycle is somewhat smaller than the load that produced it initially. The stress-softening phenomenon, also called the preconditioning effect, is widely known as the Mullins effect.

Johnson and Beatty [7] considered the material is composed of two phase (i.e. the hard phase and soft phase). Both phases are distributed uniformly throughout the material. Therefore the total length of the virgin specimen is the sum of the lengths of hard passé and soft phase, $l=l_s+l_h$. During the primary extension from the virgin state the hard phase is converted into soft phase. The conversion occurs only during primary deformation. Let ζ denote the linear fraction of hard phase present in the material in the macroscopically undeformed configuration. It follows that the remaining fraction $1-\zeta$ is the linear fraction of soft phase. The conversion of this hard phase to soft phase depends only on the maximum previous stress experienced by the hard phase.

Let microscopic uniaxial engineering strain is $\varepsilon=\lambda-1$. If we write the uniaxial engineering strain in the hard phase as $\varepsilon_h=\lambda_h-1$ and uniaxial engineering strain in the soft phase as $\varepsilon_s=\lambda_s-1$. After some small calculation the strain in the soft phase can be written as

$$\varepsilon_s = \frac{1}{1-\xi}\varepsilon \qquad (5)$$

Equation (5) can also be written as

$$\varepsilon_s = \chi\varepsilon \qquad (6)$$

where χ is the strain amplification factor.

The Mullins stress-softening effect is considered as a damage mechanism of the rubber like materials. Figure 1 shows the quasistatic loading process. As the material is first loaded along path A in figure 1(a) for $t \in [0,s_1]$, the strain response follows path A in figure 1(b). At time $t = s_1$, a stress of $\sigma(s_1) = \sigma_1$ has been reached. During the unloading from a stress of σ_1 to a stress of zero in Figure 1(a), the stress history traces path B for $t \in [s_1, s_p]$ and the corresponding strain follows path B in Figure 1(b). The material is loaded again, and the strain traces curve B in Figure 1(b) for $t \in [s_p, s_q]$ in the stress history in Figure 1(a). Finally the stress is again reduced to zero along curve F in Figure 1(a), and the strain traces curve F in Figure 1(b).

Now consider a fresh identical specimen subjected to a stress history in which the material is loaded directly to a stress σ_3 and then unloaded. The strain response during loading for our ideal model follows path ACE in Figure 1(b), and during unloading, it traces curve F. If we now load and unload this same specimen repeatedly to and from a stress σ_3, the loading and unloading strain response will each trace path F in Figure 1(b).

To illustrate the interpretation of the maximum previous stress, consider the stress history shown in figure 1 (a). For $t \in [0, s_1]$, the maximum previous stress is just the current stress, $\sigma_{max} = \sigma(t)$. On the interval $t \in [s_1, s_q]$, the maximum previous stress is $\sigma_{max} = \sigma_1$. When $t \in [s_q, s_2]$, the maximum previous stress is again the current stress$\sigma_{max} = \sigma(t)$. Thus, during a stress controlled experiment, the maximum previous stress may be a constant or a function of time.

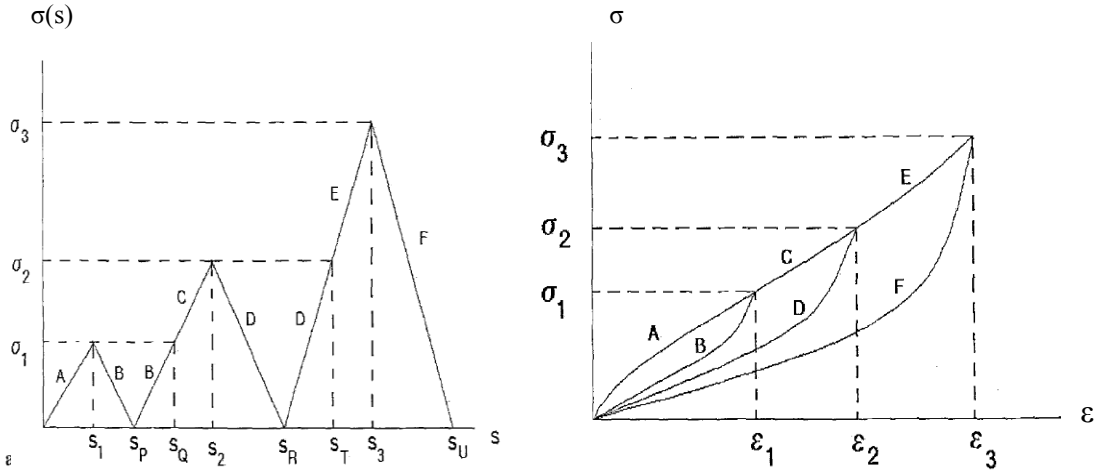

Fig: [1] Physical Description of Mullins Stress-Softening effect (a) Strain History, (b) Stress-Strain Relations [2].

Ogden [1] discussed the elastic behavior of rubber and found out how the behavior departs from the purely elastic. Johnson and Beatty [2] introduced the stress controlled experiment. In the stress controlled experiment, the uniaxial engineering stress is applied to the specimen in a predetermined manner, and the subsequent strain is measured.The constitutive equation developed by Johnson and Beatty [2], in which they investigated more closely how the outcome of the stress controlled uniaxial extension experiment can be used to get insight into the specific nature of the microstructural strain and the strain amplification functions which comprise the constitutive equation. Cheng and Chen [4] investigated experimentally the stress-stretch behavior of EPDM

rubber, Results show that the stress–stretch behavior is significantly dependent on stretching rate and the Mullins effect exists under dynamic loading.

Batra, Ghosh and Zeidman [3] proposed an integrated approach to dynamic analysis of the ring spinning process, initially they ignored the effect of air drag as well as gravitational and coriolis accelerations, and then they considered the effect of air drag. They observed that air drag is particularly useful in controlling the shape and size of the balloon.Zuniga [5] developed energy based model to characterize stress-softening effect in elastomers. They presented a new constitutive model for stress-softening for which the damage function depends on the magnitude of the energy at a material point, and then they appliedneo-Hookean model to derive stress-softened material constitutive equations.The model uses the following function defined as

$$F_s(W,W_m) = e^{-b_s\sqrt{W_m - W}} \qquad (7)$$

Johnson and Beatty [7] considered the mechanical behavior of a stress-softened material and found out that, it is necessary to introduce the idea of materials deformation history. Batra, Ghosh and Zeidman [6] discussed on the dynamics of the ring spinning process in presence of air drag, this analysis was different from previous analysis due to choice of different boundary condition, and it was more realistic.

Dorfmann and Ogden [8] presented the behavior of the hyperelastic rubber in one constitutive model (i.e. stress softening and permanent set behavior). Cantournet, Desmorat and Besson [9] explained the phenomenon of internal sliding of filled elastomers. Tang, Fraser and Wang [10] modeled the ballooning motion for ring spinning process and found out that the air drag affects the balloon tension, which in turn affects the energy consumption and yarn productivity in the ring spinning process.Sarangi, Bhattacharyya & Beatty [13] formulated the dynamical problem of a stress-softening, neo-Hookean rubber string.

III. PROBLEM FORMULATION

Constitutive relation for preconditioned string is given by Zuniga [5]. Therefore the tension- stretchrelation for a stress-softening neo-Hookean material is given by

$$P_i = \frac{AY}{3}\left(\lambda_i - \frac{1}{\lambda_i^2}\right)e^{-b\sqrt{\Theta-\theta}} \text{ where } i = 1,2 \qquad (8)$$

Where Θ defines the maximum previous strain intensity and θ is the current strain intensity which is given as

$$\Theta = \sqrt{\Lambda^4 + \frac{2}{A^2}} \quad , \quad \theta = \sqrt{\lambda_2^4 + \frac{2}{\lambda_2^2}} \qquad (9)$$

The softening compels the string to elongate more than the virgin material (i.e. the material which has never been deformed earlier) for the same load. The softening function $F(\Theta,\theta) = e^{-b\sqrt{\Theta-\theta}}$ is a function of both the maximum previous stretch and the current stretch. The maximum previous stretch in our discussion is the eyelet stretch, i.e. $\Lambda = \lambda_e$.

IV. EQUATION OF MOTION

The tension in the string is influenced by the stress-softening effect. Hence the equation of motion for the stress softened neo-Hookean string as follows

$$\frac{\partial}{\partial S_0}\left(\frac{P_1\chi_2}{\chi_1\lambda_2}e^{-b(\sqrt{\Theta-\theta_2}-\sqrt{\Theta-\theta_1})}\left(\frac{\partial \mathbf{R}_1}{\partial S_0}+\frac{\partial U}{\partial S_0}\right)\right)=$$

$$\rho A\left(\Omega^2\mathbf{e}_3\times(\mathbf{e}_3\times\mathbf{R}_1)+\Omega^2 e_3\times(e_3\times U)+2\Omega\mathbf{e}_3\times\left(\frac{\partial \mathbf{U}}{\partial\tilde{t}}\right)+\left(\frac{\partial^2\mathbf{U}}{\partial\tilde{t}^2}\right)\right)\text{-}F_D \qquad (10)$$

The following dimensionless parameters are used to normalize the equation of motion.

$$r=xe_1+ye_2+ze_3=\mathbf{R}/a,\quad \mathbf{u}=\mathbf{U}/a,\quad p=\frac{P_1}{\rho A a^2\Omega^2},$$

$$\gamma=\frac{Y}{\rho a^2\Omega^2},\quad t=\Omega\tilde{t},\quad {}^n v_{20}=\frac{{}^n V_{20}}{\Omega a},\quad d_n=\frac{16aD_n}{\rho A}$$

By using above parameters the normalized equation of motion can be derived as

$$\frac{\partial}{\partial S}\left(\frac{p\chi_2}{\chi_1\lambda_2}e^{-b(\sqrt{\Theta-\theta_2}-\sqrt{\Theta-\theta_1})}\left(\frac{\partial r}{\partial S}+\frac{\partial u}{\partial S}\right)\right)=$$

$$\left(\mathbf{e}_3\times(\mathbf{e}_3\times r)+e_3\times(e_3\times u)+2\mathbf{e}_3\times\left(\frac{\partial u}{\partial t}\right)+\left(\frac{\partial^2 u}{\partial t^2}\right)\right)+\frac{d_n}{16\lambda_1^3}\left|{}^n v_{20}\right|{}^n v_{20}, \qquad (11)$$

where ${}^n v_{20}=\frac{\partial \mathbf{r}_2}{\partial s}\times\left(\left(\frac{\partial u}{\partial t}+(\mathbf{e}_3\times\mathbf{r}_2)\right)\times\frac{\partial \mathbf{r}_2}{\partial s}\right)=(\lambda_2)^2\,{}^n v_2$

V. STEADY STATE BALLOONING MOTION

Shooting method is employed to get steady state solution. Air drag makes the motion non-planar and the planar solution can be obtained as a special case. Governing equation of motion for steady state as

$$\frac{d^2x}{ds^2}=\frac{3}{\gamma\left(1-1/\lambda_1^3\right)e^{-b\sqrt{\Theta-\theta}}}\left[\begin{array}{l}-x-\frac{\gamma}{3}\left\{\frac{3}{\lambda_1^4}e^{-b\sqrt{\Theta-\theta}}+\frac{b(1-1/\lambda_1^3)(\lambda_1^3-1/\lambda_1^3)}{\theta\sqrt{\Theta-\theta}}e^{-b\sqrt{\Theta-\theta}}\right\}\frac{dx}{ds}\frac{d\lambda_1}{ds}\\+\frac{d_n}{16\lambda_1^3}\left|{}^n v_{10}\right|\left(-y\lambda_1^2+\frac{dx}{ds}\left(\frac{dx}{ds}y-x\frac{dy}{ds}\right)\right)\end{array}\right] \qquad (12)$$

$$\frac{d^2y}{ds^2}=\frac{3}{\gamma\left(1-1/\lambda_1^3\right)e^{-b\sqrt{\Theta-\theta}}}\left[\begin{array}{l}-y-\frac{\gamma}{3}\left\{\frac{3}{\lambda_1^4}e^{-b\sqrt{\Theta-\theta}}+\frac{b(1-1/\lambda_1^3)(\lambda_1^3-1/\lambda_1^3)}{\theta\sqrt{\Theta-\theta}}e^{-b\sqrt{\Theta-\theta}}\right\}\frac{dy}{ds}\frac{d\lambda_1}{ds}\\+\frac{d_n}{16\lambda_1^3}\left|{}^n v_{10}\right|\left(x\lambda_1^2+\frac{dy}{ds}\left(\frac{dx}{ds}y-x\frac{dy}{ds}\right)\right)\end{array}\right] \qquad (13)$$

$$\frac{d^2z}{ds^2}=\frac{3}{\gamma\left(1-1/\lambda_1^3\right)e^{-b\sqrt{\Theta-\theta}}}\left[\begin{array}{l}-y-\frac{\gamma}{3}\left\{\frac{3}{\lambda_1^4}e^{-b\sqrt{\Theta-\theta}}+\frac{b(1-1/\lambda_1^3)(\lambda_1^3-1/\lambda_1^3)}{\theta\sqrt{\Theta-\theta}}e^{-b\sqrt{\Theta-\theta}}\right\}\frac{dz}{ds}\frac{d\lambda_1}{ds}\\+\frac{d_n}{16\lambda_1^3}\left|{}^n v_{10}\right|\left(\frac{dz}{ds}\left(\frac{dx}{ds}y-x\frac{dy}{ds}\right)\right)\end{array}\right] \qquad (14)$$

The above set of equations (12)-(14) is to be solved along with the tension relation

$$\frac{\gamma}{3}\left(\lambda_1^2\left(1-\frac{1}{\lambda_1^3}\right)e^{-b\sqrt{\Theta-\theta}}-\lambda_e^2\left(1-\frac{1}{\lambda_e^3}\right)e^{-b\sqrt{\Theta-\theta_e}}-\int_{\lambda_e}^{\lambda_1}\left(\xi-\frac{1}{\xi^2}\right)e^{-b\sqrt{\Theta-\theta(\xi)}}d\xi\right)=-\frac{1}{2}(x^2+y^2) \qquad (15)$$

Recall equation (8), the relation between tension and stretch without preconditioning is given as

$$\lambda_1 - \frac{1}{\lambda_1^2} = \frac{3P_1}{YA} = \frac{3p}{\gamma} \qquad (16)$$

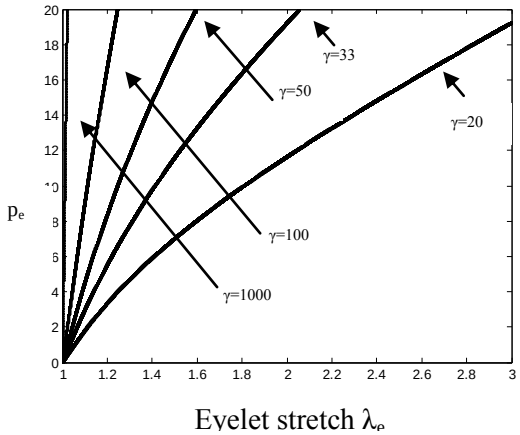

Fig.[2] Normalized Eyelet Tension Versus Eyelet Stretch of a Virgin Neo-Hookean Ballooning String in Steady State for Different Values of γ=[20,33,50,100,1000].

Figure (2) shows the variation of eyelet tension versus eyelet stretch for different values of γ, it is clearly observed in the Fig. that the stress-softening effect is predominant for lower values of γ i.e. at higher speeds. And for higher values of γ it is less significant.

V. RESULTS AND DISCUSSION

Shooting method is used in this paper to solve the planar and non planar steady state equations for γ=33 and the variation of normalized tension $p_e$with undeformed length parameter Δ_0 (=(l_0-h/l_0)) is plotted in Fig (3).

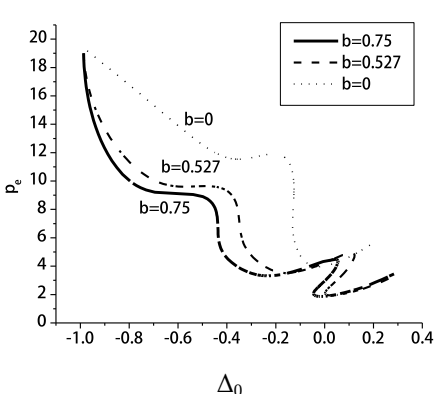

Fig: [3] Normalized eyelet tension versus string length for a Preconditioned string Λ =2, h=10, γ=33 for drag Coefficient d_n=1, softening parameter b=0.75, b=0.527 and b=0.

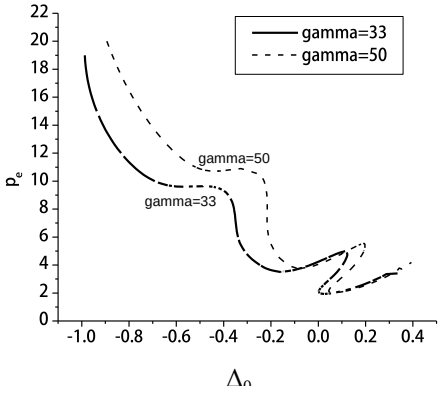

Fig: [4] Normalized eyelet tension versusstring length for a preconditioned string Λ =2, h=10, γ=50 and γ=33 for drag coefficient d_n=1, softening parameter. b=0.527

This Figure(3) shows the steady state plot of a preconditioned (stress-softened) ballooning rubber string for which the maximum previous stretch is the eyelet stretch $\Lambda = \lambda_e$ (where λ_e is fixed eyelet stretch). The stress-softened response is given by the solid and dash line for Λ =2, h=10, γ=33 d_n=1 and softening parameter b=0.75, b=0.527. The corresponding virgin response is shown by dotted line for Λ =2, h=10, γ=33 d_n=1. It is

observed from the Figure 3, that the fixed eyelet tension for the virgin cord is mostly much larger than that for the stress-softened response in the range of Δ_0 and as we increase the softening parameter (b=0.527 to b=0.75) the eyelet tension decreases for a givenΔ_0.

Figure 4 shows the variation of normalized tension p_e with normalized length parameter Δ_0 for different values of speed parameters asγ=50 and γ=33 (γ is inversely proportional to angular velocity). A hyperelastic string is tied between two eyelets and it is rotated with speeds corresponding to γ=50 and γ=33 and drag coefficient as 1 (i.e.d_n=1). It is observed that for a given value of eyelet tension the string with higher speed (i.e.γ=33) required less undeformed length and it stretches more due to high speed. Hence we can say that at higher speeds, the stress-softening effect is more.

Figure 5 shows the steady state plot for the variation of normalized tension p_e with normalized length parameter Δ_0 for different values of speeds asγ=50 and γ=33 and slightly change softening parameter b=0.75. In this Figure, it is observed that for a particular value of length parameter Δ_0 (say for example, Δ_0=-0.6), for the softening parameter b=0.527 (Fig. 4), we get fixed eyelet tension p_e=12 and 9.62 for corresponding speeds γ=50 and γ=33 and for softening parameter b=0.75 (Fig 5), we get fixed eyelet tension p_e=10.3 and 9.1. Therefore one may conclude from Fig.(4) and Fig.(5) that the softening reduces the eyelet tension for a particular Δ_0 and effect of softening is less for high speeds (i.e. for γ=50 the effect of softening is more compared to γ=33).

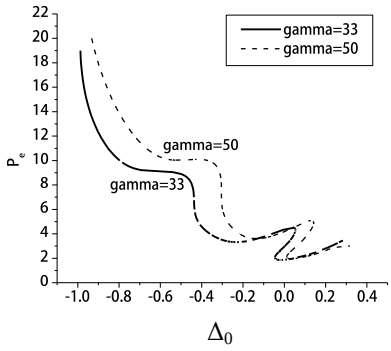

Fig: [5] Normalized Eyelet Tension Versus String Length for a Preconditioned String Λ =2, h=10, γ=50 and γ=33 for Drag Coefficient d_n=1, Softening Parameter b=0.75.

Figure 6 shows the variation of stretch of single loop balloon for normalized tension p_e=18 and corresponding virgin and stress-softened shapes are shown for different softening parameters (i.e. b=0, b=0.527. b=0.75). It is observed from steady-state curve that for any value of normalized tension p_e for which the solution corresponding to the single loop balloon, the left solution for lower value of undeformed length parameter $\Delta_0$and right solution corresponds to the higher value of undeformed length parameter Δ_0 (graph not presented here). After a certain Δ_0 the solution is governed by the right solution for single loop balloons and the string deforms more to describe larger ballooning radius. In Figure 6, it is observed that the stretches at the rotating and fixed eyelets for the virgin balloon are same irrespective of the right and left solutions. Similarly, for the stress-softened case the stretches at the left and right solutions also coincide. There is a slight difference between the values obtained in these two cases in rotating eyelet.

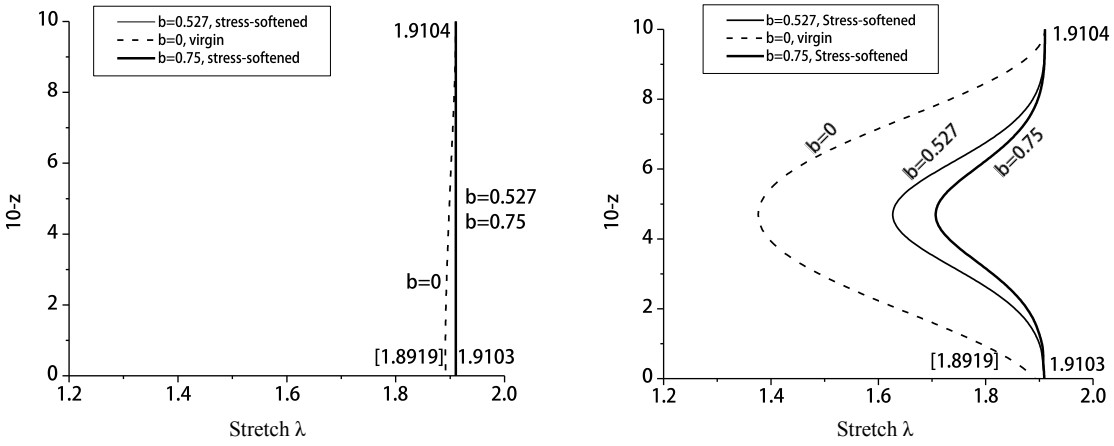

(a) **(b)**

Fig: [6] Variation of Stretch for (a) Left Solution and (b) Right Solution at P_e=18, h=10, γ=33, for Drag Coefficient d_n=0 and Softening Parameter b=0, b=0.527 and b=0.75

Figure 7 shows the variation of radial distance (r) of single loop balloon for normalized tension p_e=18 and corresponding virgin and stress-softened shapes are shown for different softening parameters (i.e. b=0, b=0.527. b=0.75). It is observed that the softened string defines the more ballooning radius as compared to that of virgin string, and the ballooning radius increases with increasing softening parameter.

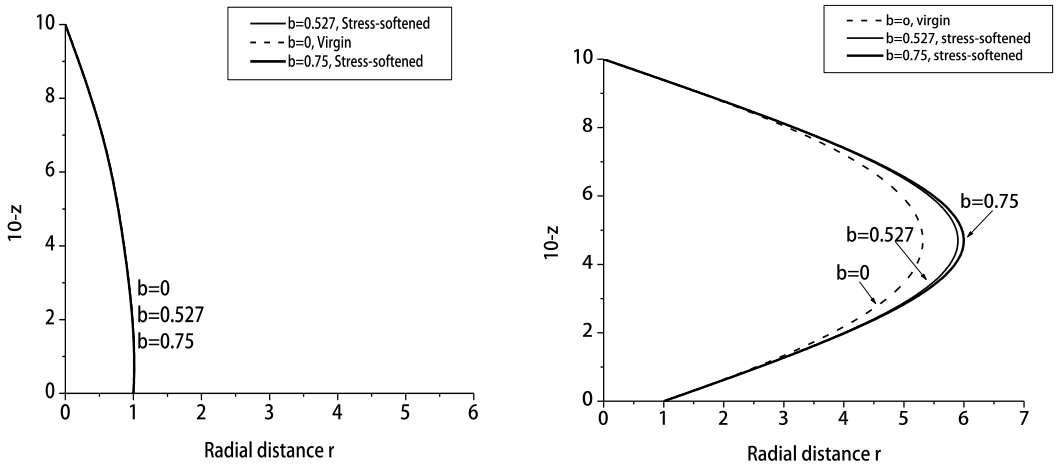

(a) **(b)**

Fig: [7] Variation of Radial Distance for (a) Left Solution and (b) Right Solution at P_e=18, h=10, γ=33, for Drag Coefficientd_n=0 and Softening Parameter b=0, b=0.527 and b=0.75.

The variation in shape of the preconditioned and virgin string with different normalized tension is shown in Figure 8. The stress-softened response is shown by solid lines where as the virgin response is shown by dashed lines. The radial distance here is the perpendicular distance measured from spindle axis at the point is represented $r = \sqrt{x^2 + y^2}$. The ordinate of the Figure at origin represents the rotating spindle end and the end of the axis represents the fixed eyelet. Earlier we observed that the stress-softened string induces more ballooning radius and subsequently it stretches more compared to the corresponding virgin case. For example, for p_e=15 the

left solution of the softened string defines the undeformed length parameter Δ_0= -0.689 (i.e. l_o=5.9206) in comparison to its corresponding virgin value as Δ_0= -0.676 (i.e. l_o=5.9665). The deformed length parameter Δ_1= 0.010 (i.e. l_1=10.1) is same for both the cases. On the other hand, for p_e=7 the softened string defines the undeformed length parameter Δ_0= 0.231 (i.e. l_o=13.004) in comparison to its corresponding virgin value as Δ_0= 0.238 (i.e. l_o=13.123). However, in this case the deformed lengths are different, i.e. the softened string deforms more to a length of l_1=15.723 in comparison to that of virgin string, which gives the value l_1=15.587. Figure shows the ballooning radius for various tensions remains almost the same for virgin and stress-softened cases.

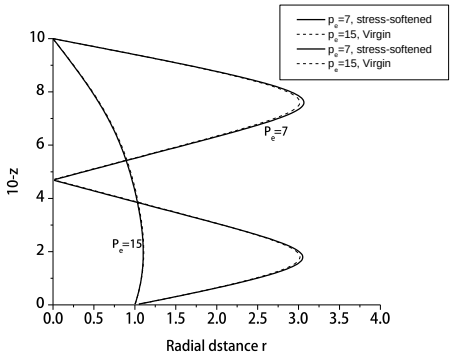

Fig:[8] Balloon shapes for a preconditioned string ʌ = λe, h=10, γ=33, d_n=0, b=0.527. For virgin and stress softened case.

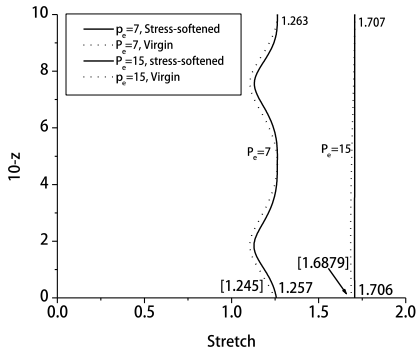

Fig:[9]Variation of stretch with height of a preconditioned string Λ = λ_e, h=10, γ=33, d_n=0, b=0.527. For virgin and stress softened case.

Figure 9 shows the variation of stretch with ballooning height for different normalized tensions. It is observed that for a particular value of normalized tension the stretch in the stress-softened string in more in comparison with virgin string. However at fixed eyelet both the stress-softened and virgin string defines the same eyelet stretch λ_e and this is the maximum stretch in the string in that perticular value of tension.

Figure 10 shows the Variation of normalized eyelet tension with eyelet stretch. Mullins effect observed theoretically in the hyperelastic ballooning rubber string in Fig (10).

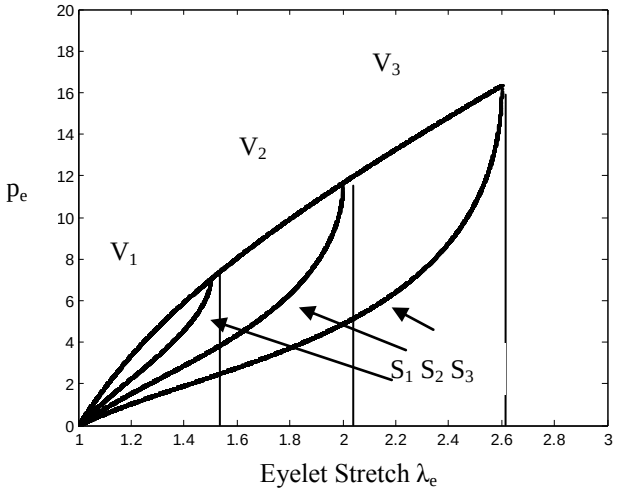

Fig.[10] Variation of Normalized Eyelet Tension with Eyelet Stretch.V is the Virgin Path and S is the Stress-Softened Path.

VI. CONCLUSIONS

Effect of stress-softening on a ballooning hyperelastic rubber string is investigated. It is found thatthe softening effect is significant for higher rotational speeds, i.e. for lower values of γ. The softening reduces the induced tension in the material and subsequently it increases the ballooning radius as compared to virgin string.

The hyperelastic material is subjected to various amount of maximum previous stretch and it is observed that the considerable softening is present only at elongations less than the previous stretch and the elongation above the maximum previous stretch is given by the virgin material response.

The present study brings some scope of future work as, effect of bending stress on ballooning motion of the rubber string, effect of twist on a ballooning string, effect of linear velocity of the yarn.

VII. ACKNOWLEDGEMENT

This research is a part of M-Tech work. The author wish to thank Professor R. Bhattacharyya, and Prof. S. Sarangi (Department of Mechanical Engineering, IIT Kharagpur).

REFERENCES

[1]. Ray W. Ogden,MECHANICS OF RUBBERLIKE SOLIDS. Dept. of MathematicsUniversity of Glasgow, 263-274 (2005).

[2]. M. A. Johnson and M. F. Beatty, A constitutive equation for the Mullins effect in stress controlled uniaxial extension experiments. Cont. Mech. Therm. 5, 301-318 (1993).

[3]. S.Batra, T. Ghosh and M.Zeidman, An integrated approach to dynamic analysis of the ring spinning process-I. Textile research Journal, 59. 309-317 (1989).

[4]. M. Cheng and W. Chen, Experimental investigation of the stress–stretch behavior of EPDM rubber with loading rate effects. Int. J. Solids and Structures. 40, 4749-4768 (2003).

[5]. A. E. Zuniga, A phenomenological energy-based model to characterize stress-softening effect in elastomers. Polymer 46, 3496-3506 (2005).

[6]. S. Batra, T. Ghosh and M. Zeidman, An integrated approach to dynamic analysis of the ring spinning process-II. Textile research Journal, 59. 416-424 (1989).

[7]. M. A. Johnson and M. F. Beatty, The Mullins effect in uniaxial extension and its influence on transverse vibration of a rubber string. Continuum Mech. Thermodyn. 5(1993), 83-115.

[8]. A. Dorfmann and Ray W. Ogden, A constitutive model for the Mullins effect with permanent set in a particle-reinforced rubber. Int. J. Solids and Structures. 42(2005) 3967-3969.

[9]. S. Cantournet , R. Desmorat, J. Besson. Mullins effect and cyclic stress softening of filled elastomers by internal sliding and friction thermodynamics model.Int. J. Solids and Structures. 46(2009) 2255-2264.

[10]. Z. X. Tang, W. B. Fraser and X. Wang, Modelling yarn balloon motion in ring spinning. Applied Mathematics Modelling 31 (2007) 1397-1410.

[11]. E. M. Arruda and M. C. Boyce, A three-dimensional constitutive model for the large stretch behavior of rubber elastic materials. J. Mech. Phys. Solids. 41,389-412 (1993).

[12]. H. M. James and E. Guth, Theory of the elastic properties of rubber. J. Chem. Phys. 10, 455-481 (1943).

[13]. S. Sarangi, R. Bhattacharyya and M. F. Beatty. Effect of Stress-softening on the Dynamics of a Load Supported by a Rubber String. J. Elasticity (2008) 92, 115-149.

[14]. W. B. Fraser, On the theory of ring spinning. Phil. Trans. R. Soc. Lond. A 342, 439-468(1993).